J. Phys. B: Atom. Molec. Phys., Vol. 8, No. 10, 1975. Printed in Great Britain.

A ten-channel eikonal treatment of differential and integral cross sections and of the (λ, χ) parameters for the $n = 2$ and 3 excitations of helium by electron impact

M R Flannery and K J McCann

School of Physics, Georgia Institute of Technology, Atlanta, Georgia 30332, USA

Received 30 January 1975

Abstract. A ten-channel eikonal treatment of the $n = 2$ and 3 collisional excitations of helium by incident electrons with energy E (eV) in the range $40 \leqslant E \leqslant 500$ is performed. Differential and integral inelastic cross sections are obtained, together with theoretical predictions of the (λ, χ) parameters which provide, as functions of scattering angle θ and E, the orientation and alignment vectors and the circular polarization fraction of the radiation emitted from the n^1P levels. The results are in satisfactory agreement with recent measurements.

1. Introduction

The study of angular correlations between the emitted photon and scattered electron in inelastic electron–atom collisions has permitted the measurement of complex transition amplitudes and atomic orientation and alignment vectors (Macek and Jaecks 1971, Fano and Macek 1973) from parameters written as λ and χ by Eminyan *et al* (1974). These collision parameters λ and χ are more basic than the total cross section σ, differential cross section $d\sigma/d\Omega$, or even percentage polarization P of the emitted radiation. They have generally been 'hidden' in most refined theoretical calculations of the collision and 'lost' in experiments designed to measure σ and P alone. By the use of delayed coincidence techniques, Eminyan *et al* (1974) have conducted striking experiments from which this basic information on λ and χ can be extracted without the need for normalization.

This work, together with the measured $d\sigma/d\Omega$ of eg Trajmar (1973) and σ of eg Donaldson *et al* (1972), all provide excellent tests of the various theoretical models recently developed for electron–atom collisions at intermediate impact energies E (see the review of McDowell 1975). For instance, in spite of its apparent success for σ and $d\sigma/d\Omega$, the Glauber approximation exhibits serious deficiencies in its predictions of λ and χ. These shortcomings are directly attributable to gross simplifications such as the assumption of a heavy particle and high-energy limit in the collision dynamics.

In this paper, the multichannel eikonal approach of Flannery and McCann (1974), which pays particular attention to the collision dynamics, is further tested by examining the variation of λ, χ, and $d\sigma/d\Omega$ with θ and E and of σ and P with E for the inelastic collisions,

$$e + He(1^1S) \rightarrow e + He(n^1L), \qquad n = 2, 3; \; L = S, P, D. \tag{1}$$

All ten channels of (1) will be closely-coupled and the accurate frozen-core Hartree–Fock wavefunctions of Cohen and McEachran (1974) will be used throughout.

2. Theory

2.1. Basic formulae

The key quantity sought by theoretical descriptions of atomic collisions is $f_{if}(\theta)$, the complex scattering amplitude as a function of scattering angle θ (in the CM frame) and of impact energy E for various i → f transitions occurring in the collision species with initial and final relative momenta $\boldsymbol{k}_i$ and $\boldsymbol{k}_f$ respectively. For a non-degenerate initial state i, experiment yields (i) the differential cross section

$$\frac{d\sigma}{d\Omega} = \frac{k_f}{k_i} \sum_{M=-L}^{L} |f_{if}^{(M)}(\theta)|^2 \tag{2}$$

summed over all degenerate magnetic substates M of the final state f of the target with angular momentum L, (ii) the associated total cross section σ and (iii) the polarization fraction P which determines the relative contribution arising from each M to the *total* σ. In a recent experiment on the 1^1S–2^1P collisional excitation of He by e, Eminyan *et al* (1974) measured, as functions of θ and E, the additional parameters

$$\lambda = \frac{|f_{if}^{(0)}|^2}{|f_{if}^{(0)}|^2 + 2|f_{if}^{(1)}|^2} \tag{3}$$

and

$$|\chi| = |\alpha_1 - \alpha_0| \tag{4}$$

where α_M is the phase of the scattering amplitude

$$f_{if}^{(M)} = |f_{if}^{(M)}| \exp(i\alpha_M) \tag{5}$$

and where the axis of quantization is taken along the incident Z direction defined by $\hat{\boldsymbol{k}}_i$.

The quantity λ is the relative contribution arising from the $M = 0$ substate to $(d\sigma/d\Omega)$ in (2), while χ is a measure of the coherence between the excitations of the $M = 0$ and 1 substates. A related quantity is the circular polarization fraction of radiation emitted perpendicular to the (assumed) XZ plane of the scattering,

$$\Pi = -2[\lambda(1-\lambda)]^{1/2} \sin\chi \equiv \overline{\Delta L_Y} \equiv L(L+1)O_1^{col} \tag{6}$$

where $\overline{\Delta L_Y}$ is the expectation value of the angular momentum transferred in the Y direction during the collision and where O_1^{col} is the orientation vector (cf Fano and Macek 1973, Eminyan *et al* 1974).

The overall accuracy of a particular theoretical collision model can therefore be assessed by the closeness between theoretical calculations and experimental measurements of the three *independent* quantities $d\sigma/d\Omega$, λ and χ as functions of θ and E. For example, the Born approximation predicts that $\lambda_B = \cos^2(\hat{\boldsymbol{K}} \cdot \hat{\boldsymbol{k}}_i)$ for S–P transitions, since $f_{if}^{(M)} \propto |Y_{1M}(\hat{\boldsymbol{K}})|^2$ is a function only of the momentum change

$$\boldsymbol{K} \equiv (K, \Theta, \Phi) = \boldsymbol{k}_i - \boldsymbol{k}_f,$$

and that $\chi_B = 0$, since $f_{if}^{(M)}$ is always real. The Π polarization is therefore zero. The prescription of Glauber (1959) involved setting $\boldsymbol{K} \cdot \boldsymbol{k}_i = 0$ so as to ease subsequent calculation with the result that $f_{if}^{(0)}$ and hence λ_G vanish. Also $\alpha_{\pm 1} = \pm i\Phi$ and so $\chi_G = 0$. By adopting a change of Z axis, however, along $\frac{1}{2}(\boldsymbol{k}_i + \boldsymbol{k}_f)$ such that K_Z in this direction

is identically zero and by following the analysis of Gerjuoy *et al* (1972), then it can be shown that, for S–P transitions, $\lambda_G = \cos^2(\hat{\boldsymbol{K}} \cdot \hat{\boldsymbol{k}}_i)$ in harmony with the first Born approximation. Therefore in spite of its relatively better performance in evaluating both σ and $d\sigma/d\Omega$, the Glauber approximation is at least worse or at best equal to the Born predictions of λ and χ. Moreover, with no simplifying assumptions made to the original six-dimensional eikonal integral, Gau and Macek (1974) have recently shown that non-zero orientation and alignment parameters can be predicted within the Glauber framework.

In the present investigation, the multichannel eikonal description (Flannery and McCann 1974) is applied to the examination of σ, $d\sigma/d\Omega$, P, λ and χ for the $n = 2$ and 3 excitations of helium by electron impact. In this treatment, the complex amplitude for scattering with final relative momentum $\boldsymbol{k}_f$ in direction (θ, ϕ) with respect to the polar axis along the direction of incident relative momentum $\boldsymbol{k}_i$ is, in the CM frame,

$$f_{if}(\theta, \phi) = -i^{\Delta+1} \int_0^\infty J_\Delta(K'\rho)[I_1(\rho, \theta) - iI_2(\rho, \theta)]\rho \, d\rho \tag{7}$$

where J_Δ are Bessel functions of integral order $(M_i - M_f)$ and where K' is the XY component $k_f \sin\theta$ of the momentum change $\boldsymbol{K} = \boldsymbol{k}_i - \boldsymbol{k}_f$. The collision functions

$$I_1(\rho, \theta; \alpha) = \int_{-\infty}^{\infty} \kappa_f(\rho, Z)\left(\frac{\partial C_f(\rho, Z)}{\partial Z}\right) \exp(i\alpha Z) \, dZ \tag{8}$$

and

$$I_2(\rho, \theta; \alpha) = \int_{-\infty}^{\infty} \left(\kappa_f(\kappa_f - k_f) + \frac{\mu}{\hbar^2} V_{ff}\right) C_f(\rho, Z) \exp(i\alpha Z) \, dZ \tag{9}$$

contain a dependence on the scattering angle θ via

$$\alpha = k_f(1 - \cos\theta) = 2k_f \sin^2 \tfrac{1}{2}\theta \tag{10}$$

the difference between the Z component of the momentum change $\boldsymbol{K}$ and the minimum change $k_i - k_f$ in the collision. The coupling amplitudes C_f are solutions of the following set of N coupled differential equations

$$\frac{i\hbar^2}{\mu}\kappa_f(\rho, Z)\frac{\partial C_f(\rho, Z)}{\partial Z} + \left(\frac{\hbar^2}{\mu}\kappa_f(\kappa_f - k_f) + V_{ff}(\rho, Z)\right) C_f(\rho, Z)$$

$$= \sum_{n=1}^{N} C_n(\rho, Z) V_{fn}(\rho, Z) \exp i(k_n - k_f)Z, \qquad f = 1, 2, \ldots, N \tag{11}$$

solved subject to the asymptotic boundary condition $C_f(\rho, -\infty) = \delta_{if}$. The local wavenumber of relative motion at separation $\boldsymbol{R} \equiv (R, \Theta, \Phi) \equiv (\rho, \Phi, Z)$ is

$$\kappa_n(\boldsymbol{R}) = \left(k_n^2 - \frac{2\mu}{\hbar^2} V_{nn}(\boldsymbol{R})\right)^{1/2}$$

where the interaction matrix elements

$$V_{nm}(\boldsymbol{R}) = \langle \psi_n(\boldsymbol{r}_1, \boldsymbol{r}_2) | V(\boldsymbol{r}_1, \boldsymbol{r}_2, \boldsymbol{R}) | \psi_m(\boldsymbol{r}_1, \boldsymbol{r}_2) \rangle$$

connect the various electronic states $\psi_n(\boldsymbol{r}_1, \boldsymbol{r}_2)$ of atomic helium and where V is the instantaneous e–He electrostatic interaction. In the uncoupled limit, the elastic scattering in each channel is described by the eikonal approximation to scattering by the

corresponding static (diagonal) interaction $V_{nn}(\boldsymbol{R})$ rather than by the instantaneous interaction $V(\boldsymbol{R}, \boldsymbol{r}_1, \boldsymbol{r}_2)$, (as is the case in Glauber's treatment of elastic scattering). It can be shown directly that, at high energies, the basic equations satisfy the optical theorem,

$$\sum_f \sigma_{if} = \frac{4\pi}{k_i} \operatorname{Im} f_{ii}(0) \equiv 4\pi \int_0^\infty (\operatorname{Re} C_i - 1)\rho \, d\rho = 2\pi \sum_f \int_0^\infty |C_f - \delta_{if}|^2 \rho \, d\rho. \tag{12}$$

Verification, however, for all impact energies is not as straightforward and would require explicit numerical evaluation of all the cross sections.

2.2. *Wavefunctions and interactions*

All ten channels of (1) will be closely coupled. We adopt the frozen-core Hartree–Fock $n = 1$–3 helium wavefunctions of Cohen and McEachran (1974) in the form

$$\psi_{1s,nlm}(\boldsymbol{r}_1, \boldsymbol{r}_2) = N_{nl}[\phi_0(\boldsymbol{r}_1)\phi_{nlm}(\boldsymbol{r}_2) + \phi_0(\boldsymbol{r}_2)\phi_{nlm}(\boldsymbol{r}_1)] \tag{13}$$

in which the frozen, inner 1s orbital is (in au)

$$\phi_0(\boldsymbol{r}) = 2^{5/2} \, e^{-2r} Y_{00}(\hat{\boldsymbol{r}}) \tag{14}$$

and the orbital for the second electron in state (nlm) is rewritten (in au) as

$$\phi_{nlm}(\boldsymbol{r}) = \sum_{N=l+1}^{J-l} B_N^{nl} \, e^{-\beta r} r^{N-1} Y_{lm}(\hat{\boldsymbol{r}}), \qquad \beta = \frac{2}{n} \tag{15}$$

where J is the maximum number of linear coefficients B_N^{nl} given in terms of Cohen and McEachran's original parameters a_j^{nl} by

$$B_N^{nl} = \sum_{j=N+l}^{J} \frac{(-1)^{N-l} 2^l (j!)^2 (2\beta)^{N-l-1}}{(N-l-1)!(j-N-l)!(N+l)!} a_j^{nl}, \qquad N = 1, 2, \ldots, J. \tag{16}$$

The above transformation (16) facilitates subsequent evaluation of the e–He interaction matrix elements

$$V_{ij}(\boldsymbol{R}) = \langle \phi_i(\boldsymbol{r}_1, \boldsymbol{r}_2) \left| -\frac{2}{R} + \frac{1}{|\boldsymbol{R} - \boldsymbol{r}_1|} + \frac{1}{|\boldsymbol{R} - \boldsymbol{r}_2|} \right| \phi_j(\boldsymbol{r}_1, \boldsymbol{r}_2) \rangle \tag{17}$$

as analytical functions of $\boldsymbol{R}$ such that the exponential and linear parameters α_i and a_s in the resulting expression,

$$V_{nlm,n'l'm'}(\boldsymbol{R}) = \sum_{L=|l-l'|}^{(l+l')} \left[-\frac{a_{-t}}{R^t} + \sum_{i=1}^{2} e^{-\alpha_i R} \sum_{s=-t}^{16} a_s R^s \right] Y_{LM}(\boldsymbol{R}) \tag{18}$$

can be determined exactly and automatically.

2.3. *Test of wavefunctions*

Theoretical refinement to the collision model must be accompanied whenever possible by accurate atomic wavefunctions since the goodness thereby introduced by the former may be completely swamped by an inappropriate choice of wavefunctions (cf McCann and Flannery 1974). The overall reliability of the present set of wavefunctions has already been gauged by examination of associated eigenenergies and cusp conditions (Cohen and McEachran 1967, McEachran and Cohen 1969). In this investigation, the present set of wavefunctions did reproduce the accurate Born results of Bell *et al* (1969)

for the $n = 2$ and 3 excitations of He. However, it is worth noting that similar reproductions were achieved for the $n = 4$–6 He excitations only when one adopted additional linear parameters a_j^{nl}, which were not contained in the above cited references (so as to economize in table presentation), but which were obtained from Cohen and McEachran (1974) privately. Therefore, in all the present calculations we have employed the twenty-parameter functions provided by Cohen and McEachran (1974). The non-orthogonality integrals $\langle \Psi_i | \Psi_f \rangle$ were found to be negligible for all channels.

3. Results and discussion

A ten-channel eikonal description (7)–(11) was carried out for the inelastic collisions

$$e + He(1^1S) \rightarrow e + He(n^1L), \qquad n = 2, 3;\ L = S, P, D \tag{19}$$

and the parameters $d\sigma/d\Omega$, λ and χ determined from (2)–(5) as functions of scattering angle θ for various impact energies E(eV) in the range $40 \leqslant E \leqslant 500$. A four-channel ($1^1S$, 3^1S, $3^1P_{0,\pm1}$) treatment was also performed.

3.1. Total cross sections and polarization fractions

Total excitation cross sections

$$\sigma(E) = 2\pi \frac{k_f}{k_i} \int_0^\pi |f_{if}(\theta)|^2 \, d(\cos\theta) \tag{20}$$

are displayed in figures 1–4 for each transition in (19), together with comparison experimental and theoretical data. These figures include results from the following recent theories:

(i) The second-order potential treatments (S) of Berrington *et al* (1973) for the $n = 2$ excitations and of Bransden and Issa (1975) for the $n = 3$ excitations,
(ii) The second-order diagonalization procedure of Baye and Heenen (1974),
(iii) The first-order many-body approach (M) of Thomas *et al* (1974) for the $n = 2$ excitations,
(iv) A four-channel eikonal (E4) study (McCann and Flannery 1974) of the $n = 2$ excitations,
(v) The Glauber treatment of Chan and Chen (1973, 1974a, b) for the $n = 2$ and 3^1P excitations,
(vi) The Born results (B) of Bell *et al* (1969).

The experimental data are taken from Brongsmera *et al* (1972), Trajmar (1973), Rice *et al* (1972), Vriens *et al* (1968), Miller *et al* (1968), Donaldson *et al* (1972), de Jongh and van Eck (1971) and Moustafa Moussa *et al* (1969). Since figures 1–4 provide a rather detailed comparison, only a few comments are needed. In general, the present ten-channel results (E10) are in good accord with experiment down to 50 eV, below which the scatter in the various measurements preclude any definition. Couplings with the $n = 3$ channels are very important for the 2^1S excitation at all energies, and couplings with the $n = 2$ channels influence the 3^1S excitation appreciably, although the corresponding 2^1P and the 3^1P cross sections are essentially left unaffected. The 2^1P distorted Born wave results (not shown) of Madison and Shelton (1973) are indistinguishable from the present E10 curve. Cross sections in excess of the Born values are obtained

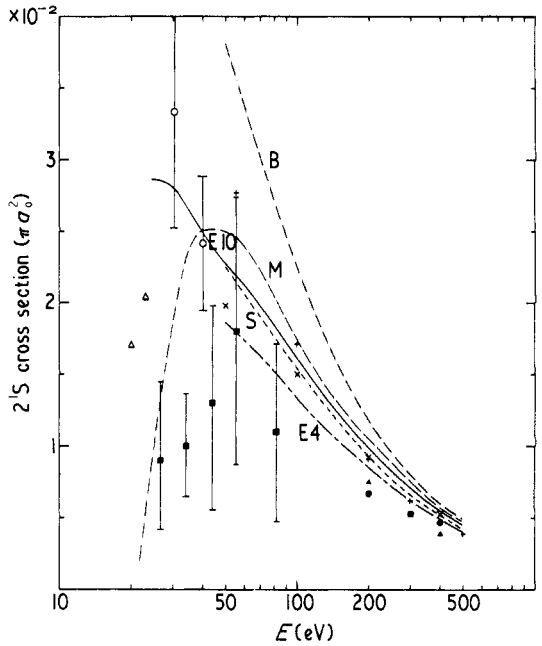

Figure 1. Total cross section for the 1^1S–2^1S transition in He by collision with electrons of energy E(eV). Theory: E10, E4, present ten- and four-channel eikonal treatments, respectively; S, second-order potential method with simple set of wavefunctions (Berrington *et al* 1973); M, first-order many-body approach (Thomas *et al* 1974); B, Born approximation (Bell *et al* 1969); ×, second-order diagonalization method (Baye and Heenen 1974); + Glauber approximation (Chan and Chen 1973, 1974a). Experiment: ■, Rice *et al* (1972); ▲, Miller *et al* (1969); ●, Vriens *et al* (1968); ⊙, Trajmar (1973); △, Brongsmera *et al* (1972).

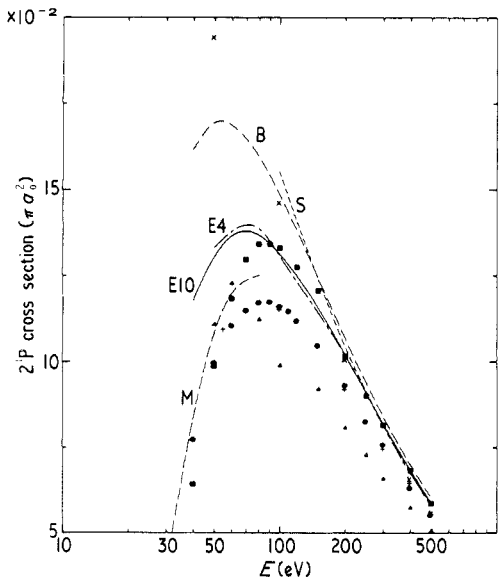

Figure 2. Total cross section for the 1^1S–2^1P transition in He by collision with electrons of energy E(eV). Theory: exactly as in figure 1. Experiment: ●, Donaldson *et al* (1972); ■, de Jongh and van Eck (1971); ▲, Moustafa Moussa *et al* (1969).

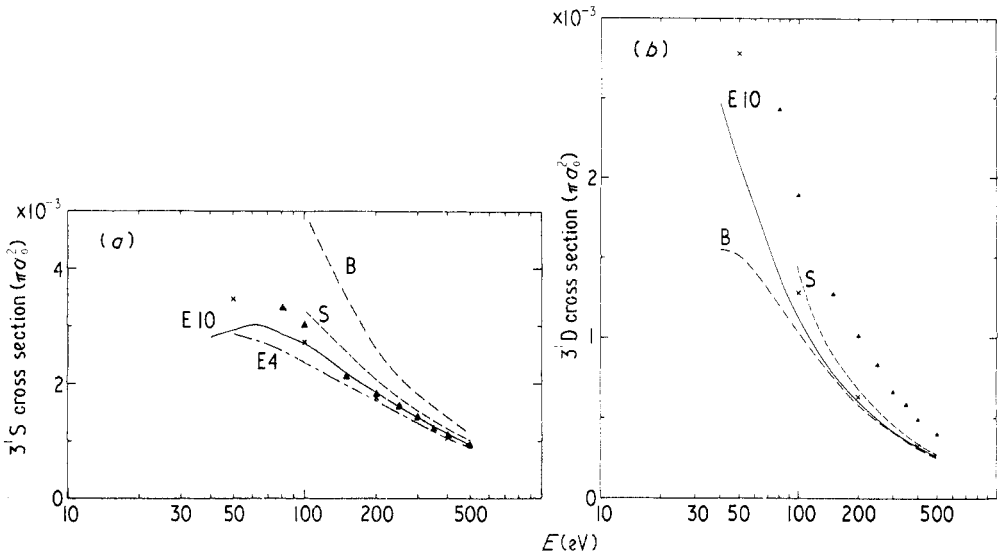

Figure 3. Total cross section for excitation of the (*a*) $3\,^1S$, (*b*) $3\,^1D$ states of He by collision with electrons of energy E(eV). Theory: as in figure 1 except S, second-order potential method (Bransden and Issa 1975). Experiment: ▲, Moustafa Moussa *et al* (1969).

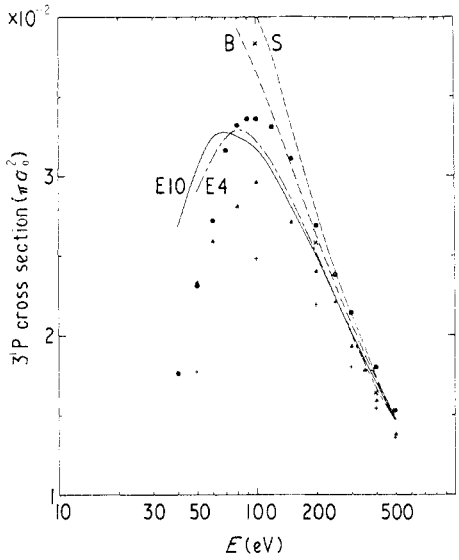

Figure 4. Total cross section for the 1^1S–3^1P transition in He by collision with electrons of energy E(eV). The symbols are as in figure 3.

only for the 3^1D excitation in figure 3(*b*), when the 3^1P–3^1D dipole coupling becomes extremely important and causes the large enhancement at the lower energies. Note that the Born limit remains unattained even at 500 eV for the n^1S excitations in figures 1 and

3(*a*), although the n^1P and 3^1D cross sections show fairly rapid convergence from below and above respectively onto the corresponding Born limits.

The present ten-channel cross sections σ_M for excitation of magnetic sublevel M of (19) are presented in table 1 together with the four-channel and Born values at 500 eV. The percentage polarization fractions

$$P(n^1P) = \frac{\sigma_0 - \sigma_1}{\sigma_0 + \sigma_1} \tag{21}$$

and

$$P(3^1D) = \frac{3(\sigma_0 + \sigma_1 - 2\sigma_2)}{5\sigma_0 + 9\sigma_1 + 6\sigma_2} \tag{22}$$

for the radiation emitted from the n^1P and n^1D states respectively (Percival and Seaton 1958) are displayed in table 2. For high $E \geqslant 300$ eV, $P(2^1P) \simeq P(3^1P)$.

Detailed Balance. In the course of a related investigation on a ten-channel treatment of excitation to the $n = 3$ states and de-excitation to the 1^1S state in e–He(2^1S) collisions, the superelastic cross section $\sigma(2^1S–1^1S)$ was obtained. The principle of detailed balance

$$E_f\sigma_{fi}(2^1S–1^1S\,;\,E_f) = E_i\sigma_{if}(1^1S–2^1S\,;\,E_i)$$

between the excitation and de-excitation cross sections evaluated at the energies E_i and E_f respectively, corresponding to the appropriate channel, was found to be closely satisfied numerically. Moreover, this procedure provided the following additional two cross sections for the $1^1S–2^1S$ excitation: $2{\cdot}87 \times 10^{-2}\pi a_0^2$ and $2{\cdot}82 \times 10^{-2}\pi a_0^2$, $E_i = 25{\cdot}6$ eV and 30·6 eV, respectively, which would have required lengthy computing time if calculated directly. Figure 1 includes these two lowest energy points, in agreement with the measurements of Trajmar (1973).

3.2. Differential cross sections

These provide a more sensitive test of the present theory and representative cases are displayed in figures 5–7 for the various excitations as a function of scattering angle θ at two incident energies as indicated. (Computer printouts of the remainder at all the energies in table 1 are available from the authors upon request.)

Examination of figures 5 and 6 shows that the present multichannel model is generally quite successful in describing inelastic scattering about the forward direction up to $\theta \simeq 40°$. In particular, as indicated by figure 5(*a*) the many-body treatment of Thomas *et al* (1974) fails quite markedly, by comparison, to reproduce the measurements of Trajmar (1973) in this angular range for the 2^1S excitation. This shortcoming is presumably attributed to the fact that their first-order approach has neglected the $2^1S–2^1P$ dipole coupling which strongly enhances the 2^1S scattering about the forward direction. The 2^1P cross section is affected much less by the presence of this coupling, as shown by figure 6. With increasing E, the scattering becomes more concentrated in the forward direction and is therefore well described by the present model.

Although the present version of the multichannel eikonal approximation is clearly invalid for backward scattering, calculations were nevertheless performed for the full angular range $0 \leqslant \theta \leqslant 180°$ so as to illustrate certain inadequacies of the treatment. Its failure to properly describe large angle scattering in figures 5 and 6 is a direct result of the *explicit* neglect of electron exchange—some of which, however, is *implicitly*

Table 1. Total excitation cross sections (in units of $10^{-2}\pi a_0^2$) given by a ten-channel treatment of the processes $e + He(1^1S) \rightarrow e + He(n^1L)$ at incident electron energies E(eV).

E(eV) \ nL	2^1S	2^1P_0	$2^1P_{\pm1}$	2^1P	3^1S	3^1P_0	$3^1P_{\pm1}$	3^1P	3^1D_0	$3^1D_{\pm1}$	$3^1D_{\pm2}$	3^1D
40	2·45	6·92	4·86	11·78	2.89^{-1}†	1·83	0·85	2·68	1.11^{-1}	1.12^{-1}	2.46^{-2}	2.48^{-1}
50	2·27	6·95	6·09	13·04	2.93^{-1}	1·89	1·15	3·04	8.38^{-2}	9.55^{-2}	2.95^{-2}	2.09^{-1}
60	2·12	6·77	6·89	13·66	3.02^{-1}	1·86	1·38	3·24	6.92^{-2}	8.04^{-2}	3.24^{-2}	1.82^{-1}
80	1·84	6·18	7·50	13·68	2.86^{-1}	1·65	1·60	3·25	4.70^{-2}	5.75^{-2}	3.39^{-2}	1.38^{-1}
100	1·61	5·52	7·60	13·12	2.69^{-1}	1·48	1·69	3·17	3.56^{-2}	4.31^{-2}	3.36^{-2}	1.12^{-1}
150	1·22	4·34	7·22	11·56	2.18^{-1}	1·12	1·69	2·81	2.10^{-2}	2.63^{-2}	3.01^{-2}	7.74^{-2}
200	9.86^{-1}	3·54	6·67	10·21	1.84^{-1}	8.96^{-1}	1·60	2·50	1.50^{-2}	1.85^{-2}	2.66^{-2}	6.01^{-2}
300	7.07^{-1}	2·50	5·69	8·19	1.40^{-1}	6.22^{-1}	1·40	2·02	9.40^{-3}	1.08^{-2}	2.13^{-2}	4.15^{-2}
400	5.49^{-1}	1·81	5·02	6·83	1.12^{-1}	4.49^{-1}	1·25	1·70	6.83^{-3}	7.35^{-3}	1.77^{-2}	3.19^{-2}
500	4.49^{-1}	1·31	4·54	5·85	9.24^{-2}	3.30^{-1}	1·13	1·46	5.52^{-3}	5.39^{-3}	1.52^{-2}	2.61^{-2}
500‡	4.46^{-1}	1·20	4·66	5·86	8.71^{-2}	3.12^{-1}	1·15	1·46	—	—	—	—
500§	4.84^{-1}	—	—	6·02	1.09^{-1}	—	—	1·49	—	—	—	2.51^{-2}

† Superscript denotes the power of 10 by which the entry must be multiplied.

‡ Four-channel treatment ($1^1S\ n^1S\ n^1P_{0,\pm1}$).

§ Born (Bell *et al* 1969).

Table 2. Polarization fractions of the radiation emitted from He(n^1L).

E(eV) \ n^1L	2^1P	3^1P	3^1D
40	0·480	0·624	0·377
50	0·391	0·533	0·327
60	0·326	0·459	0·287
80	0·245	0·347	0·211
100	0·185	0·273	0·149
150	0·092	0·140	0·039
200	0·030	0·057	−0·030
300	−0·065	−0·059	−0·122
400	−0·162	−0·164	−0·179
500	−0·268	−0·263	−0·215

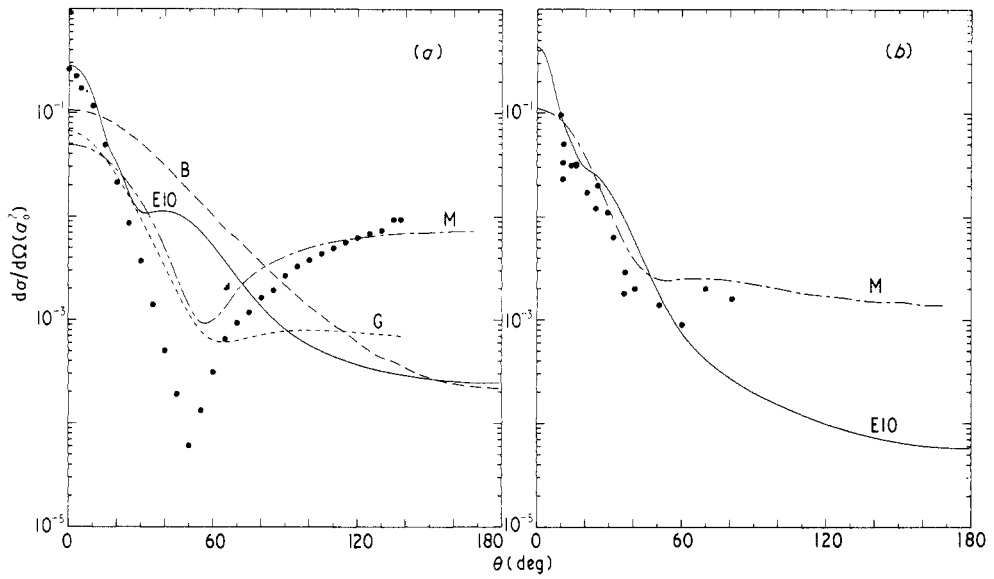

Figure 5. Differential cross sections for the 2^1S excitation of He by electrons with energy (*a*) 40 eV, (*b*) 80 eV. Theory: E10, present ten-channel eikonal treatment; M, first-order many-body approach (Thomas *et al* 1974); G, B, Glauber and Born approximations (see Trajmar 1972). Experiment: ●, (*a*) Trajmar (1973), (*b*) Rice *et al* (1972).

included by virtue of the multistate expansion—and by the adoption of a straight line trajectory so as to ease computation of both the eikonal (or phase distortion to the relative motion) in each channel and of the transition amplitudes C_n coupling the various channels. The Glauber and Born approaches also suffer from these defects. These effects, however, can be incorporated directly within the basic eikonal model, although a combination of a full quantal partial-wave analysis of the close encounters responsible for these effects and a multichannel eikonal method for the more distant encounters is perhaps a better alternative. There is, however, recent evidence (Bransden and Winters 1975, McDowell *et al* 1975, Winters 1974) that inclusion of exchange may be

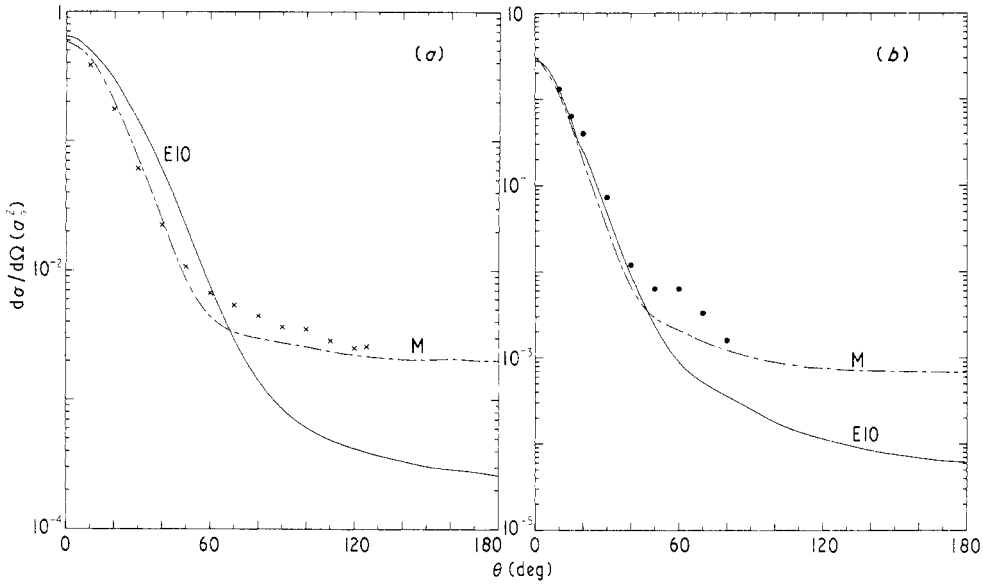

Figure 6. Differential cross sections for the 2^1P excitation of He by electrons with energy (*a*) 40 eV, (*b*) 80 eV. Theory: as in figure 5. Experiment: ×, Hall *et al* (1973); ●, Truhlar *et al* (1970).

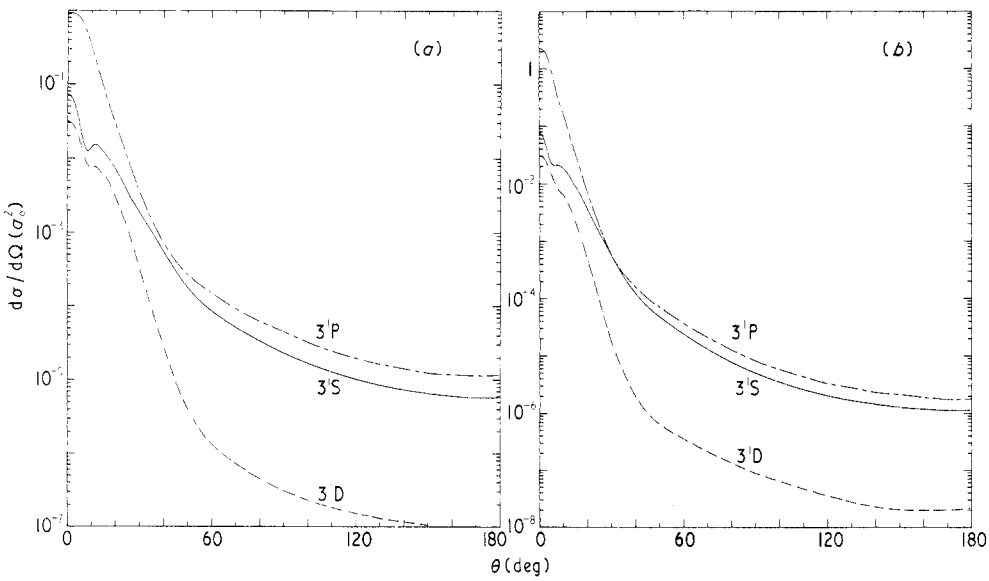

Figure 7. Ten-channel differential cross section for the 3^1S, 3^1P and 3^1D excitations of He by electrons with energy (*a*) 100 eV, (*b*) 200 eV.

insufficient to reproduce large-angle inelastic scattering; a proper account of distortion in the final channel together with a consistent treatment of exchange polarization may also be necessary. The contribution arising from these larger scattering angles to the

total excitation cross section is, however, extremely small, such that the present treatment which includes all of the major effects needed for an accurate description of scattering through small angles, less than 50°, provides accurate integral cross sections.

Differential cross sections for the $n = 3$ excitations are displayed in figure 7 at higher impact energies E and are similar in shape to the corresponding $n = 2$ excitations. The n^1P_0 excitation ($\Delta = 0$) decreases from a non-zero value for scattering in the forward direction $\theta = 0$. The $n^1P_{\pm 1}$ excitations ($\Delta = \pm 1$) increase from zero, reach a maxima at θ_c (which shifts towards smaller angles and becomes larger than the corresponding n^1P_0 cross sections at θ_c as E is increased) and decreases faster than the n^1P_0 excitation. While this behaviour is not apparent in the differential cross section for the total n^1P excitation, it is nevertheless reflected by slight structure in the n^1S and n^1D excitations via intermediate couplings with the $n^1P_{0,\pm 1}$ substates. Thus this structure apparent in figures 5 and 7 does not originate from the same effects which yield the minimum obtained by the first-order many-body treatment (cf figure 5).

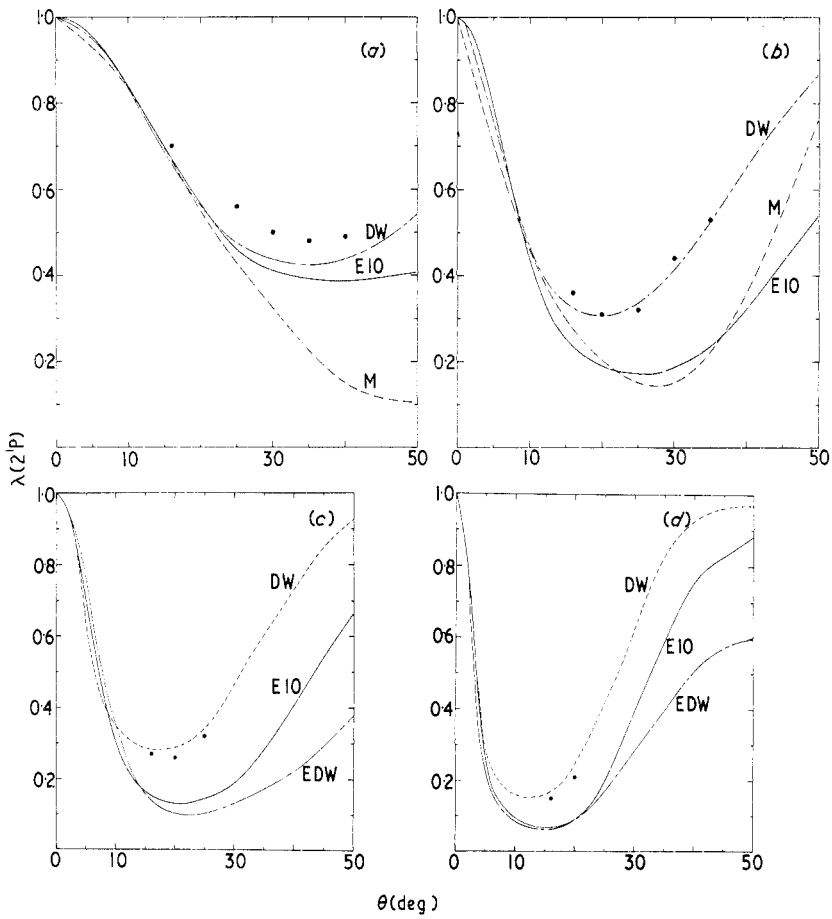

Figure 8. Variation of $\lambda(2^1P)$ with scattering angle θ at impact energies (*a*) 40 eV, (*b*) 80 eV, (*c*) 100 eV and (*d*) 200 eV. E10, present ten-channel treatment: DW, distorted-wave Born approximation (Madison and Shelton 1973): EDW, eikonal DW (Joachain and Vanderpoorten 1974); M, first-order many-body approach (Thomas *et al* 1974); ●, Eminyan *et al* (1974).

3.3. λ, χ and circular polarization

In figures 8 and 9 the present predictions of $\lambda(2^1P)$ and $\lambda(3^1P)$ obtained from equation (3) are compared with the measurements of Eminyan *et al* (1974, 1975) and with the available distorted wave and many-body calculations. Agreement with experiment is good, particularly at the smaller scattering angles. Measurements, however, are not available for scattering by $\theta \leqslant 15°$, an angular region for which the present multichannel eikonal treatment is particularly successful (cf figures 5 and 6). It is also worth noting that the goodness of the many-body treatment of the 2^1P total and differential excitation (cf figures 2 and 6) is not maintained for $\lambda(2^1P)$ at the larger scattering angles. Figure 9 demonstrates that the relative agreement between the present approach and measurements becomes improved for the 3^1P excitation, especially at the smaller scattering angles. The apparent structure in $\lambda(3^1P)$ is somewhat reproduced, although shifted to larger scattering angles. There are no other theoretical values available for comparison. After the present λ curves reach their minima at angles θ which decrease with increasing E, they tend monotonically toward unity as $\theta \to 180°$.

The present variation of λ with E and θ is presented in figure 10. Since λ denotes the relative contribution arising from the $M = 0$ sublevel to the 2^1P differential cross section,

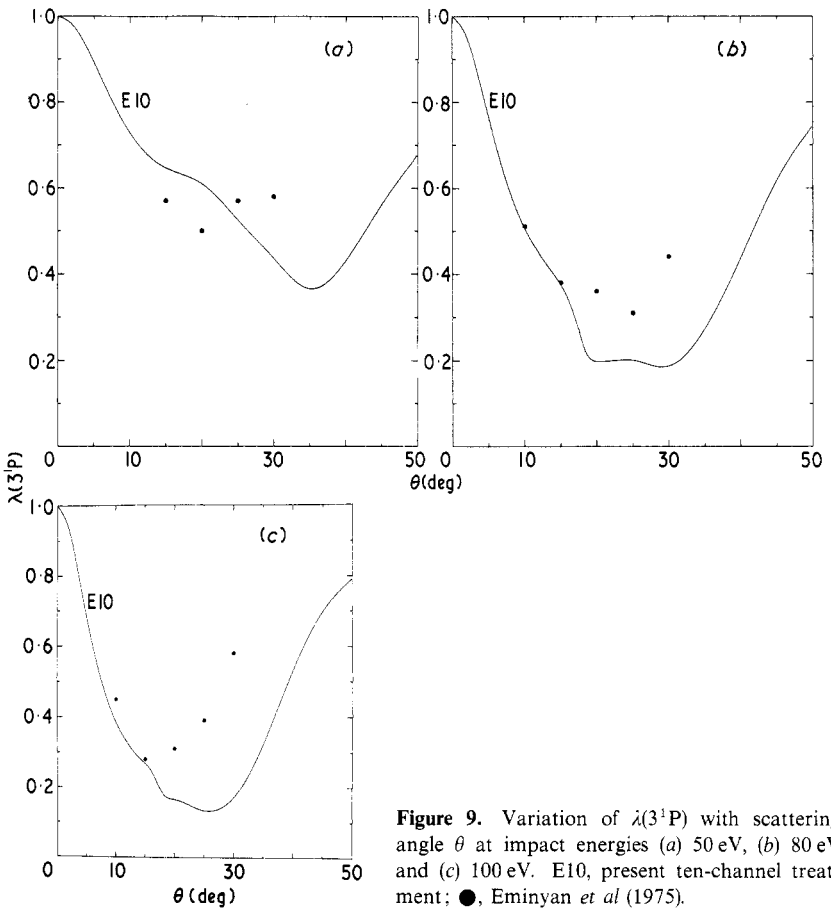

Figure 9. Variation of $\lambda(3^1P)$ with scattering angle θ at impact energies (*a*) 50 eV, (*b*) 80 eV and (*c*) 100 eV. E10, present ten-channel treatment; ●, Eminyan *et al* (1975).

figure 10 shows quite clearly that for scattering through $\theta \leqslant 20°$, excitation of the $M = \pm 1$ substates dominates with increasing E, except in the near vicinity of the forward direction $\theta = 0$ when only $\Delta M = 0$ transitions occur. The small-angle region $\theta \leqslant 20°$ contributes most to the total cross section which is therefore primarily controlled by $M = \pm 1$ excitations at high impact energies (cf table 1). For scattering through larger angles (past the λ minima), the trend is reversed with excitation of the $M = 0$ sublevel dominating at high E, although here its relative contribution to the total cross section is negligible.

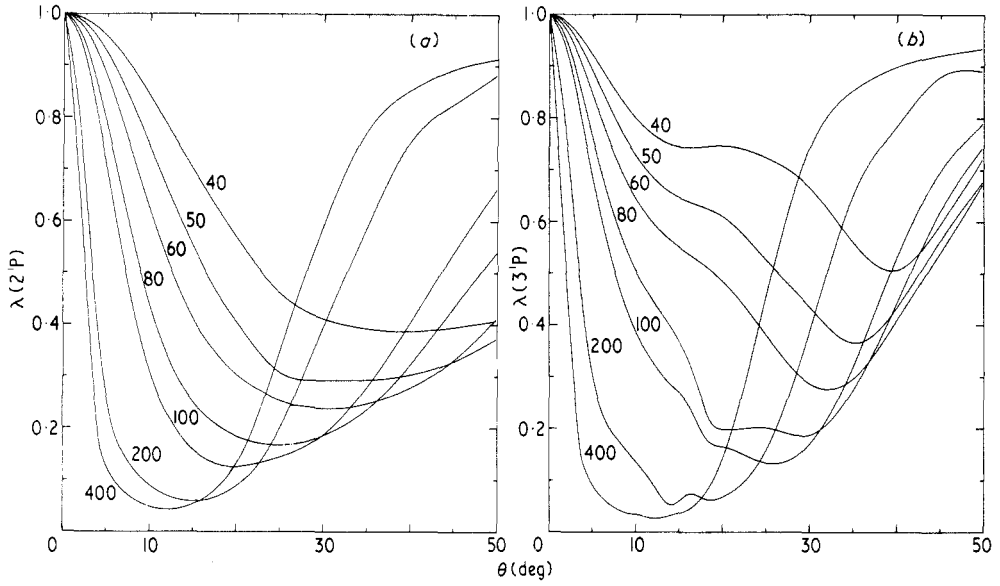

Figure 10. Present variation of (*a*) $\lambda(2^1\mathrm{P})$ and (*b*) $\lambda(3^1\mathrm{P})$ with scattering angle θ, and with impact energy E(eV), indicated on each curve.

The parameter $|\chi|$ which is a measure of the coherence between the excitations of the $M = 0$ and ± 1 sublevels (or phase difference between the corresponding oscillating and rotating dipoles, respectively) is displayed in figures 11 and 12 for transitions to the $2^1\mathrm{P}$ and $3^1\mathrm{P}$ levels. The $2^1\mathrm{P}$ measurements are bracketed by the distorted wave and the present ten-channel eikonal results. The figures 11(*c*) and (*d*) show that both eikonal models yield χ values in closer accord with experiment than does the DWBA which, however, provides better agreement for λ. Also, in spite of the fact that Joachain and Vanderpoorten (1974) obtained somewhat improved agreement of χ with experiment when the distorting potentials in the initial and final channels were taken to be the (local) Glauber optical potentials (rather than the customary target static potentials, which yield χ smaller than those shown in the figures), the present refinements to the basic eikonal model has introduced, in general, even closer agreement with experiment. In figure 12, the weak structure in $\chi(3^1\mathrm{P})$ is reproduced, although at somewhat larger angles, and the agreement improves as E increases to 100 eV.

The variation of χ (which is negative) with θ and E is displayed in figure 13. For high E and small θ, χ tends to zero in harmony with the prediction of Born's approximation, although for intermediate energies $E \leqslant 100$ eV, a non-zero limit is attained. When

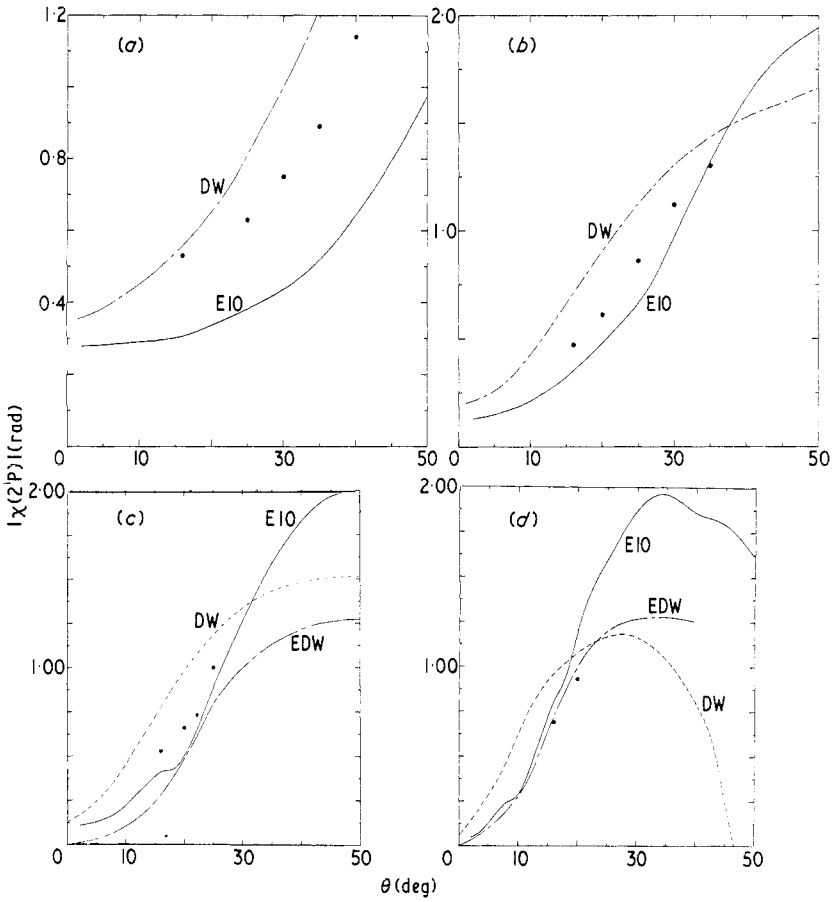

Figure 11. Variation of $|\chi(2^1P)|$ with scattering angle θ at impact energies (*a*) 40 eV, (*b*) 80 eV, (*c*) 100 eV and (*d*) 200 eV. E10, present ten-channel treatment; DW, distorted-wave Born approximation (Madison and Shelton 1973); EDW, eikonal DW (Joachain and Vanderpoorten 1974); ●, Eminyan *et al* (1974).

χ passes through $\frac{1}{2}\pi$ ie when the phases of the oscillating and rotating dipoles differ by $\frac{1}{2}\pi$, and, provided that the magnitudes of the corresponding amplitudes are about equal (ie $\lambda \simeq 0{\cdot}5$), then at this particular scattering angle θ_c, fully circularly polarized light would be observed in a direction at right angles to the plane of scattering.

The departure from equal population of the $M = 0$ and ± 1 states at θ_c is obtained from figure 10 and hence circularly polarized light will be observed for scattering angles whose shift from θ_c depends on the function $\lambda(\theta)$. The fraction Π of circularly polarized radiation emitted perpendicular to the XZ plane of scattering is the following combination

$$\Pi(\theta, E) = -2[\lambda(1-\lambda)]^{1/2} \sin\chi \tag{23}$$

of λ and χ. Figure 14 displays the present variation of Π with θ and E. Fully circularly polarized light (ie $\Pi = 1$) is in evidence only for low-energy, large-angle collisions. For scattering in the forward direction, Π is small and almost independent of E. The recognition that Π is also $\overline{\Delta L_Y}$, the angular momentum transferred in a direction Y perpendicular to the assumed XY plane or scattering, provides some further insight to figure 14.

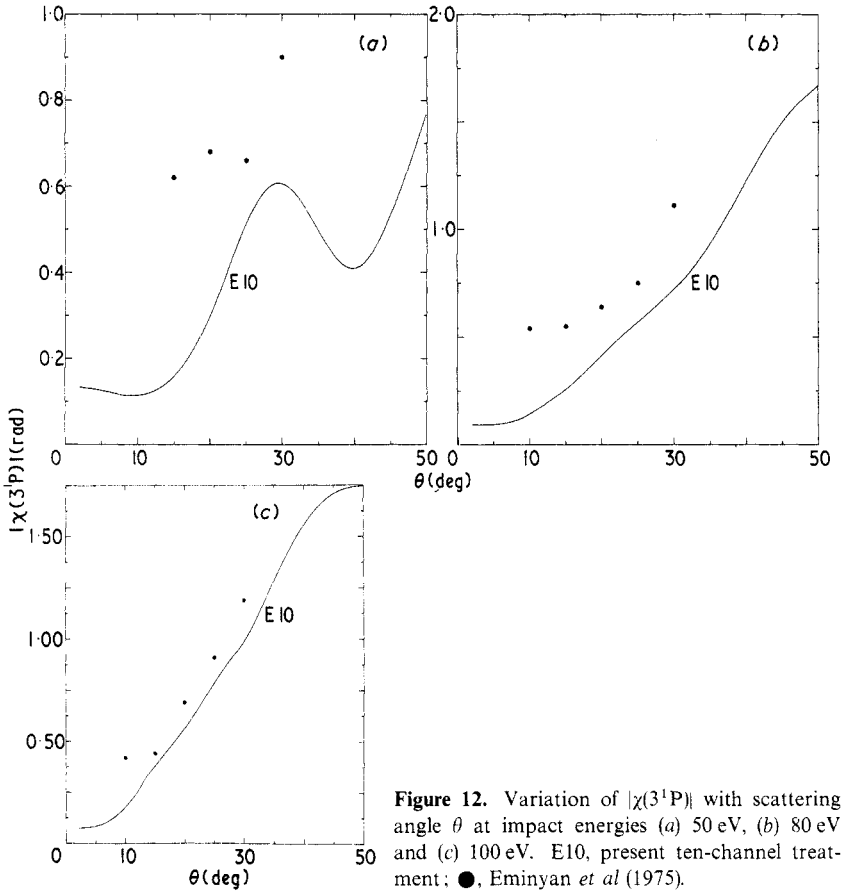

Figure 12. Variation of $|\chi(3^1P)|$ with scattering angle θ at impact energies (*a*) 50 eV, (*b*) 80 eV and (*c*) 100 eV. E10, present ten-channel treatment; ●, Eminyan *et al* (1975).

In the impulsive high-energy limit, the torque $\boldsymbol{N}$ about an origin O due to a force $\boldsymbol{F}$ acting on an electron at position vector $\boldsymbol{r}(x, y, z)$ for time Δt is, from classical mechanics,

$$\boldsymbol{N} = \boldsymbol{r} \times \boldsymbol{F} = \frac{\Delta \boldsymbol{L}}{\Delta t} \tag{24}$$

and hence the Y component of the angular momentum change ΔL is

$$\Delta L_Y = [\langle \boldsymbol{r} \rangle \times \Delta \boldsymbol{P}]_Y = 2k_i \sin \tfrac{1}{2}\theta \langle z \rangle \tag{25}$$

where $\Delta \boldsymbol{P}$ is the linear momentum $2k_i \sin\frac{1}{2}\theta$ transferred and $\langle \boldsymbol{r} \rangle$ is some time average of $\boldsymbol{r}$ during the impulsive encounter. Small-angle collisions with an atom result from distant encounters, and the target atom and hence $\langle z \rangle$ remains essentially unaffected. Thus $\overline{\Delta L}_Y$ increases as $E^{1/2}$ and θ, until sufficiently large E and θ when large-angle, close-encounter collisions dominate, such that the expectation value $\langle z \rangle$ must decrease more rapidly than $E^{1/2} \sin \frac{1}{2}\theta$ so as to cause the decreasing $\overline{\Delta L}_Y$ observed in figure 13.

In conclusion, the present version of the multichannel eikonal treatment provides a successful description of inelastic collisions at intermediate and high impact energies. Its success for total excitation cross sections can be attributed to the fact that here the small-angle scattering ($\theta \leqslant 50°$) which dominates the total cross section even at low energies ($E \simeq 40$ eV) is well described. The main effects, such as intermediate (long-range) couplings between each channel, some polarization of each target state, and

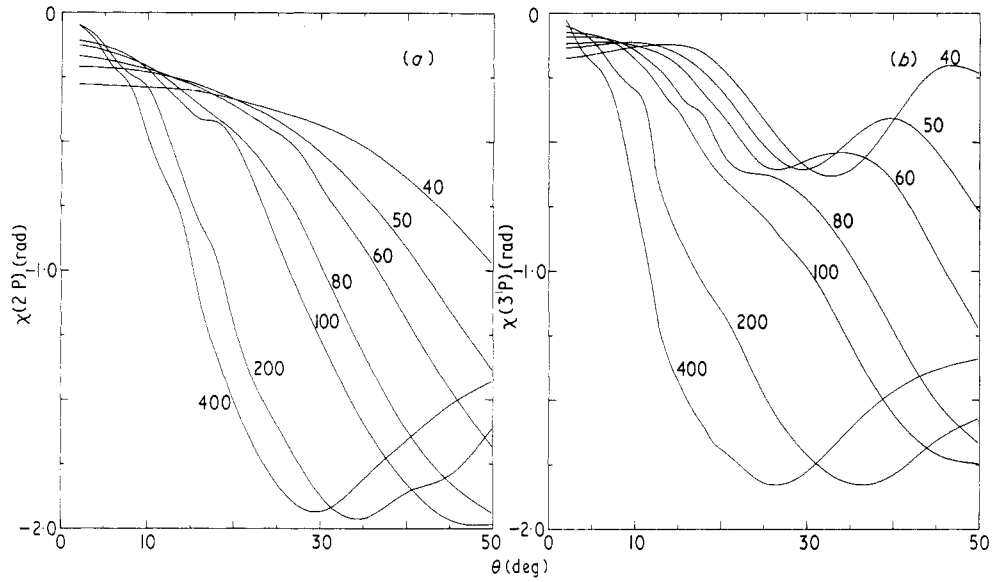

Figure 13. Present variation of (*a*) $\chi(2^1P)$ and (*b*) $\chi(3^1P)$ radians with scattering angle θ and with impact energy E(eV) indicated on each curve.

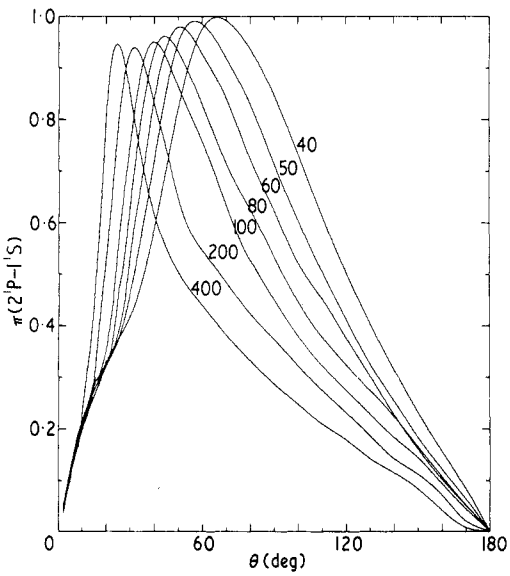

Figure 14 The variation of the fraction π of circularly polarized radiation, emitted from $He(2^1P)$ and observed at right angles to the scattering plane, with scattering angle θ and with impact energy E(eV) indicated on each curve.

static distortion in each channel needed for a correct description of small-angle scattering are included. Also the multichannel eikonal expansion ensures (i) that convergence in partial-wave contributions is always attained especially in the high-energy limit, (ii) that the long-range couplings can affect distant encounters (or large total angular momentum), and also (iii) that some account of electron exchange is provided. More basic parameters

such as λ (which yields the relative contribution of the $M = 0$ excitation to the differential cross section) and χ (which is the phase difference between the $M = 0$ and ± 1 scattering amplitudes) are also well described as functions of E and θ, particularly at the smaller scattering angles.

Acknowledgments

The authors wish to thank Professors M Cohen and R P McEachran for sending us a full tabulation of their wavefunctions. Also preprints sent by Professors B H Bransden, M R C McDowell and H Kleinpoppen before publication are all gratefully acknowledged. This research was sponsored by the Air Force Aerospace Research Laboratories, Air Force Systems Command, United States Air Force, Contract F 33615-74-C-4003.

References

Baye D and Heenen P-H 1974 *J. Phys.* B: *Atom. Molec. Phys.* **7** 938–49
Bell K L, Kennedy D J and Kingston A E 1969 *J. Phys.* B: *Atom. Molec. Phys.* **2** 26–43
Berrington K A, Bransden B H and Coleman J P 1973 *J. Phys.* B: *Atom. Molec. Phys.* **6** 436–49
Bransden B H and Issa M R 1975 *J. Phys.* B: *Atom. Molec. Phys.* **8** 1088–94
Bransden B H and Winters K H 1975 *J. Phys.* B: *Atom. Molec. Phys.* **8** 1236–44
Brongsmera H H, Knoop F W E and Backx C 1972 *Chem. Phys. Lett.* **13** 16–9
Chan, F T and Chen S T 1973 *Phys. Rev.* A **8** 2191–4
—— 1974a *Phys. Rev.* A **9** 2393–7
—— 1974b *Phys. Rev.* A **10** 1151–6
Cohen M and McEachran R P 1967 *Proc. Phys. Soc.* **92** 37–41
—— 1974 private communication
Donaldson F G, Hender M A and McConkey J W 1972 *J. Phys.* B: *Atom. Molec. Phys.* **5** 1192–210
Eminyan M, MacAdam K B, Slevin J and Kleinpoppen H 1974 *J. Phys.* B: *Atom. Molec. Phys.* **7** 1519–42
Eminyan M, MacAdam K B, Slevin J, Standage M and Kleinpoppen H 1975 *J. Phys.* B: *Atom. Molec. Phys.* **8** in press
Fano U and Macek J H 1973 *Rev. Mod. Phys.* **45** 533–73
Flannery M R and McCann K J 1974 *J. Phys.* B: *Atom. Molec. Phys.* **7** 2518–32
Gau J N and Macek J 1974 *Phys. Rev.* A **10** 522–38
Gerjuoy E, Thomas B K and Sheorey V B 1972 *J. Phys.* B: *Atom. Molec. Phys.* **5** 321–33
Glauber R J 1959 *Lectures in Theoretical Physics* vol 1, ed W E Brittin and L G Dunham (New York: Interscience) p 369
Hall R I, Joyez G, Mazean J, Reinhardt J and Schermann C 1973 *J. Phys., Paris* **34** 827–43
Joachain C J and Vanderpoorten R 1974 *J. Phys.* B: *Atom. Molec. Phys.* **7** L528–30
de Jongh J P and van Eck J 1971 *Proc. 7th Int. Conf. on Physics of Electronic and Atomic Collisions* (Amsterdam: North-Holland) Abstracts pp 701–3
McCann K J and Flannery M R 1974 *Phys. Rev.* A **10** 2264–72
McDowell M R C 1975 *Proc. Int. Symp. on Electron and Photon Interactions with Atoms* ed H Kleinpoppen and M R C McDowell (New York: Plenum Press)
McDowell M R C, Morgan L A and Myerscough V P 1975 *J. Phys.* B: *Atom. Molec. Phys.* **8** 1053–72
McEachran R P and Cohen M 1969 *J. Phys.* B: *Atom. Molec. Phys.* **2** 1271–3
Macek J and Jaecks D H 1971 *Phys. Rev.* A **7** 2288–300
Madison D H and Shelton W N 1973 *Phys. Rev.* A **7** 499–513
Miller K J, Mielczarek S R and Krauss M 1968 *J. Chem. Phys.* **51** 945–57
Moustafa Moussa H R, de Heer F J and Schulten J 1969 *Physica* **40** 517–49
Percival I C and Seaton M J 1958 *Phil. Trans. R Soc.* A **251** 113–38
Rice J K, Truhlar D G, Cartwright D C and Trajmar S 1972 *Phys. Rev.* A **5** 762–82
Thomas L D, Csanak G, Taylor H S and Yarlagadda B S 1974 *J. Phys.* B: *Atom. Molec. Phys.* **7** 1719–33
Trajmar S 1973 *Phys. Rev.* A **8** 191–203
Truhlar D G, Rice J K, Kupperman A, Trajmar S and Cartwright D C 1970 *Phys. Rev.* A **1** 778–802
Vriens L, Simpson J A and Mielczarek S R 1968 *Phys. Rev.* **165** 7–15
Winters K H 1974 *PhD Thesis* University of Durham